Protein Engineering

Deutsche Ausgabe: DOI: 10.1002/ange.201603652
Internationale Ausgabe: DOI: 10.1002/anie.201603652

Accelerating the Association of the Most Stable Protein–Ligand Complex by More than Two Orders of Magnitude

*Christoph Giese, Jonathan Eras, Anne Kern, Martin A. Schärer, Guido Capitani, and Rudi Glockshuber**

Abstract: *The complex between the bacterial type 1 pilus subunit FimG and the peptide corresponding to the N-terminal extension (termed donor strand, Ds) of the partner subunit FimF (DsF) shows the strongest reported noncovalent molecular interaction, with a dissociation constant (K_D) of 1.5×10^{-20} M. However, the complex only exhibits a slow association rate of $330\,M^{-1}s^{-1}$ that limits technical applications, such as its use in affinity purification. Herein, a structure-based approach was used to design pairs of FimGt (a FimG variant lacking its own N-terminal extension) and DsF variants with enhanced electrostatic surface complementarity. Association of the best mutant FimGt/DsF pairs was accelerated by more than two orders of magnitude, while the dissociation rates and 3D structures of the improved complexes remained essentially unperturbed. A K_D value of 8.8×10^{-22} M was obtained for the best mutant complex, which is the lowest value reported to date for a protein/ligand complex.*

Proteins and their ligands associate with very diverse rates. Specifically, experimentally determined association rate constants (k_{on}) of natural protein–protein complexes span multiple orders of magnitude, ranging from about 10^3 to $10^{10}\,M^{-1}s^{-1}$.[1] The upper end of this scale is given by the theoretical, diffusion-limited rate constant of 10^9–$10^{10}\,M^{-1}s^{-1}$ that is predicted for the collision of uniformly reactive spheres of equal size.[2] The necessity for two proteins to collide with the correct relative orientation prior to formation of the final complex, however, often lowers this upper k_{on} limit to values of about 10^4–$10^6\,M^{-1}s^{-1}$.[1b,3] This effect can be compensated by electrostatic surface complementarity between the binding partners favoring a pre-orientation upon collision that facilitates formation of the final complex.[1c,4] A classic example is the association between the ribonuclease barnase and its inhibitor barstar, which is characterized by the rate-limiting, electrostatically driven formation of an early recognition complex that is followed by fast conformational rearrangements generating the final, specific complex.[4b] Rational optimization of electrostatic attraction between proteins has been used successfully to generate variants of protein–protein complexes with increased association rates.[5]

Herein, we probed the principle of electrostatic surface complementarity to accelerate the association between a folded protein and intrinsically disordered peptides. As a model system, we used the complex between the *Escherichia coli* type 1 pilus subunit FimG and the 15-residue peptide corresponding to the N-terminal extension of its partner subunit FimF (DsF). The FimG/DsF complex is the thermodynamically and kinetically most stable, noncovalent protein–ligand complex reported to date.[6] The interaction between FimG and DsF follows the mechanism of donor strand complementation, in which the incomplete, immunoglobulin-like fold of every pilus subunit is completed by an N-terminal extension, termed donor strand (Ds), of the following subunit.[7] This type of interaction leads to virtually infinite stability of the pilus against spontaneous dissociation and unfolding.[6b] The bimolecular complex between FimGt, an N-terminally truncated FimG variant lacking its own donor strand, and the DsF peptide has a dissociation constant (K_D) of 1.5×10^{-20} M. The interaction is dominated by an extremely low dissociation rate (k_{off}) of $5\times10^{-18}\,s^{-1}$ which can only be observed when FimGt unfolds in conjunction with peptide release.[6] Nevertheless, the association of FimGt with DsF proved to be slow ($k_{on}=330\,M^{-1}s^{-1}$) compared to most natural protein–protein or protein–peptide complexes, which is likely a consequence of the fact that pilus subunit association is catalyzed by the assembly platform FimD in vivo.[8] Our approach for improving the k_{on} value of the FimGt/DsF complex through amplified electrostatic attraction was based on the crystal structure of the complex (Figure 1). FimGt has 5 basic and 10 acidic residues (theoretical pI = 4.5). None of the basic but two of the acidic residues, Asp26 and 29 on the A″-strand of FimGt, are close to the DsF binding site. The charged side chains in the DsF sequence are two aspartates (Asp2, Asp13) and two solvent-exposed arginine residues (Arg8, Arg12). Arg8 of DsF is in close proximity to Asp26 of FimGt, and Arg12 of DsF is close to Asp29 of FimGt (Figure 1).

Based on these charge distributions, we decided to make FimGt even more acidic and DsF more basic. To avoid interference with structure or stability of the complex we restricted amino acid replacements to solvent-exposed residues. Regarding the DsF peptide, its basic character was gradually increased by replacing Thr4 and Thr6 by arginine and by removing the negative charge of Asp13, resulting in the three variants DsF^{T4R}, $DsF^{T4R\text{-}T6R}$, and $DsF^{T4R\text{-}T6R\text{-}D13N}$. Far-UV CD spectroscopy confirmed that the free peptides are completely unstructured in solution (see Figure S1 in the

[*] Dr. C. Giese, J. Eras, A. Kern, Prof. R. Glockshuber
Department of Biology
ETH Zurich
Otto-Stern-Weg 5, 8093 Zürich (Switzerland)
E-mail: rudi@mol.biol.ethz.ch
Dr. M. A. Schärer, Dr. G. Capitani
Laboratory of Biomolecular Research, Paul Scherrer Institute
5232 Villigen-PSI (Switzerland)

Supporting information for this article can be found under: http://dx.doi.org/10.1002/anie.201603652.

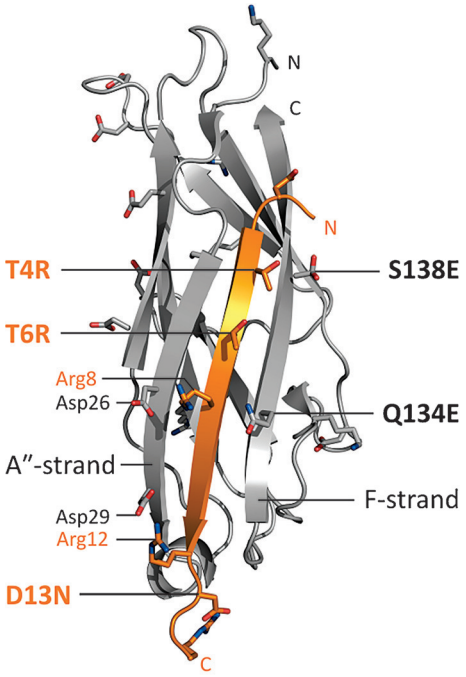

Figure 1. Engineering strategy to accelerate the association of FimGt with DsF. The crystal structure of the FimGt/DsF WT complex (PDB code 3BFQ) is shown with FimGt in gray and the DsF peptide in orange.[6b] The side chains of charged residues are shown as a stick model. Amino acid substitutions in FimGt and/or DsF tested for association rate enhancement are indicated in bold.

Supporting Information). In the FimGt/DsF wild type (WT) complex, the DsF peptide is inserted between the N-terminal A″ strand and the C-terminal F strand of FimGt and forms 20 intermolecular β-sheet hydrogen bonds with strands A″ and F.[6b] As the F strand lacks charged residues, it appeared more attractive than the A″ strand for introducing additional negative charges in FimGt. Consequently, Gln134 and Ser138 of FimGt were replaced by glutamate, alone or in combination, yielding the three protein variants FimGt^{Q134E}, FimGt^{S138E}, and FimGt$^{Q134E\text{-}S138E}$.

We measured the association rate constants for all possible protein/peptide combinations at low ionic strength (11 mM), utilizing a decrease of about 10% in the intrinsic tryptophan fluorescence of FimGt upon DsF binding (Figure S2). For the FimGt/DsF WT complex, we obtained $k_{on} = (278 \pm 6)\ M^{-1}\,s^{-1}$ with this method, which is in good agreement with the value of $330\ M^{-1}\,s^{-1}$ determined earlier using an interrupted binding assay that unambiguously monitored complex formation.[6a] Thus, the decrease in FimGt fluorescence upon DsF binding directly reported the formation of the complex. The binding kinetics were measured under pseudo-first-order conditions ($\geq$5-fold excess of DsF over FimGt). All pseudo-first-order rate constants linearly increased with DsF concentration (Figure S3), demonstrating that the bimolecular peptide binding reactions were always rate-limiting for complex formation and that the amino acid substitutions in FimGt and DsF did not change the reaction mechanism. Consequently, all k_{on} values could be obtained by global fitting of the pseudo-first-order kinetics according to an irreversible second-order reaction (Figure S3).

Figure 2 and Table 1 summarize the measured k_{on} values. Overall, all mutant FimGt/DsF complexes showed higher k_{on} values than the WT complex. The two complexes which associated fastest, FimGt^{Q134E}/DsF$^{T4R\text{-}T6R\text{-}D13N}$ and FimGt$^{Q134E\text{-}S138E}$/DsF$^{T4R\text{-}T6R\text{-}D13N}$, showed k_{on} values of $(1.38 \pm 0.03) \times 10^4\ M^{-1}s^{-1}$ and $(2.52 \pm 0.05) \times 10^4\ M^{-1}s^{-1}$, corresponding to a 50- and 91-fold faster association compared to the WT complex, respectively.

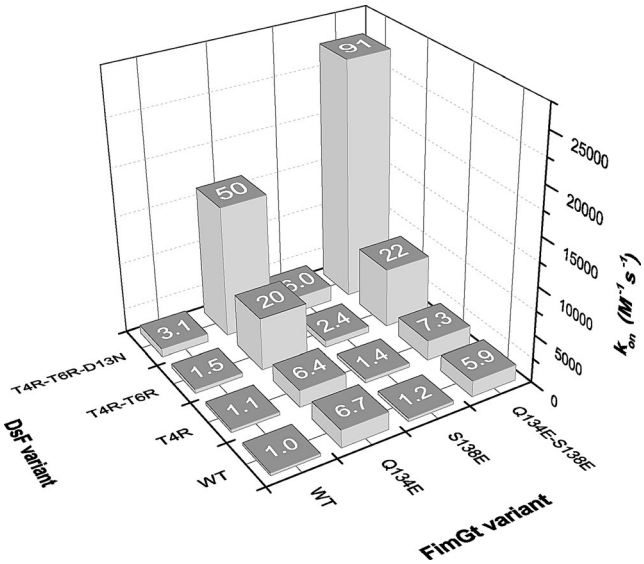

Figure 2. Association rate constants of FimGt/DsF variant pairs at pH 8.0, 25 °C. Acceleration factors ($k_{on}/k_{on(WT)}$) are indicated on top of each column.

Comparison of the measured k_{on} values of the individual, mutant FimGt/DsF pairs showed that the introduction of a single negative charge at position 134 of FimGt already led to 7-fold faster binding of the DsF WT peptide. In contrast, association of FimGt^{S138E} with DsF WT was not accelerated. The double mutant FimGt$^{Q134E\text{-}S138E}$ bound DsF WT as fast as FimGt^{Q134E}, indicating that the two replacements affected the association with DsF WT independently. This also showed that the specific location of newly introduced charges is more important for rate acceleration than the total charge of FimGt, which is in line with results obtained for other protein–protein complexes with improved association rates.[5b,c] An analogous result was obtained for the DsF variants, where the T4R substitution had no effect on the association with any of the FimGt variants. Introduction of a second positive charge into DsF increased the association rate 2–3-fold, but only in combination with the acidified FimGt variants, and the third replacement D13N led to 2–4-fold higher rate constants compared to DsF$^{T4R\text{-}T6R}$.

The association kinetics of FimGt WT with DsF WT were previously found to be essentially independent of ionic strength between zero and 1 M (Figure S4; Ref. [6a]), showing that electrostatic interactions do not contribute to the k_{on} value of the WT complex. In contrast, a strong depend-

Table 1: Kinetic and thermodynamic parameters for the association and dissociation/unfolding of the different FimGt/DsF complexes.[a]

FimGt variant	DsF variant	DsF amino acid sequence	k_{on} [$M^{-1}s^{-1}$][c]	k_{off} [s^{-1}][d]	m_U [M^{-1}][e]	K_D [M]
WT[b]	WT[b]	ADSTITIRGYVRDNG	278 ± 6	$(5.0\pm0.17)\times10^{-18}$	4.18 ± 0.15	$(1.80\pm0.06)\times10^{-20}$
	T4R	ADS**R**ITIRGYVRDNG	306 ± 6	$(9.2\pm2.7)\times10^{-17}$	3.80 ± 0.05	$(3.0\pm0.9)\times10^{-19}$
	T4R-T6R	ADS**R**I**R**IRGYVRDNG	405 ± 8	$(6.0\pm2.6)\times10^{-18}$	4.27 ± 0.07	$(1.5\pm0.6)\times10^{-20}$
	T4R-T6R-D13N	ADS**R**I**R**IRGYVR**N**NG	$(8.6\pm0.2)\times10^{2}$	$(1.7\pm0.4)\times10^{-17}$	4.14 ± 0.04	$(2.0\pm0.5)\times10^{-20}$
Q134E	WT	ADSTITIRGYVRDNG	$(1.85\pm0.04)\times10^{3}$	$(2.9\pm1.1)\times10^{-17}$	3.92 ± 0.06	$(1.6\pm0.6)\times10^{-20}$
	T4R	ADS**R**ITIRGYVRDNG	$(1.78\pm0.04)\times10^{3}$	$(1.3\pm0.5)\times10^{-17}$	4.14 ± 0.06	$(7.3\pm2.8)\times10^{-21}$
	T4R-T6R	ADS**R**I**R**IRGYVRDNG	$(5.5\pm0.1)\times10^{3}$	$(8.1\pm3.1)\times10^{-17}$	3.89 ± 0.06	$(1.5\pm0.6)\times10^{-20}$
	T4R-T6R-D13N	ADS**R**I**R**IRGYVR**N**NG	$(1.38\pm0.03)\times10^{4}$	$(3.4\pm0.8)\times10^{-17}$	4.03 ± 0.04	$(2.4\pm0.6)\times10^{-21}$
S138E	WT	ADSTITIRGYVRDNG	326 ± 7	$(1.2\pm0.6)\times10^{-17}$	4.01 ± 0.07	$(3.8\pm1.7)\times10^{-20}$
	T4R	ADS**R**ITIRGYVRDNG	383 ± 8	$(3.4\pm1.1)\times10^{-17}$	3.98 ± 0.05	$(8.8\pm2.7)\times10^{-20}$
	T4R-T6R	ADS**R**I**R**IRGYVRDNG	$(6.7\pm0.1)\times10^{2}$	$(1.5\pm0.7)\times10^{-16}$	3.78 ± 0.07	$(2.3\pm1.0)\times10^{-19}$
	T4R-T6R-D13N	ADS**R**I**R**IRGYVR**N**NG	$(1.67\pm0.03)\times10^{3}$	$(1.7\pm0.4)\times10^{-17}$	4.13 ± 0.04	$(1.0\pm0.2)\times10^{-20}$
Q134E-S138E	WT	ADSTITIRGYVRDNG	$(1.64\pm0.03)\times10^{3}$	$(3.0\pm1.5)\times10^{-17}$	3.91 ± 0.08	$(1.8\pm0.9)\times10^{-20}$
	T4R	ADS**R**ITIRGYVRDNG	$(2.03\pm0.04)\times10^{3}$	$(2.5\pm0.9)\times10^{-17}$	4.02 ± 0.06	$(1.2\pm0.5)\times10^{-20}$
	T4R-T6R	ADS**R**I**R**IRGYVRDNG	$(6.2\pm0.1)\times10^{3}$	$(7.3\pm2.6)\times10^{-17}$	3.88 ± 0.06	$(1.2\pm0.4)\times10^{-20}$
	T4R-T6R-D13N	ADS**R**I**R**IRGYVR**N**NG	$(2.52\pm0.05)\times10^{4}$	$(2.2\pm0.5)\times10^{-17}$	4.11 ± 0.04	$(8.8\pm2.0)\times10^{-22}$
	SRIRIRGYVR	S**R**I**R**IRGYVR	$(7.8\pm0.2)\times10^{4}$	$(1.3\pm0.3)\times10^{-14}$	3.62 ± 0.04	$(1.7\pm0.4)\times10^{-19}$

[a] Parameters recorded at pH 8.0, 25 °C. Errors are standard errors obtained from the respective fits. The standard errors for the k_{on} values were all between 0.05 and 0.4%. As individual rate constants could only be reproduced within an error of 2%, all k_{on} values are given with 2% error. New residues introduced into the DsF sequences are depicted in bold. [b] Values of k_{off} and m_U for the FimGt/DsF WT complex were taken from References [6a,b], respectively. [c] Values of k_{on} were deduced from the kinetics of tryptophan fluorescence decrease upon DsF binding (see Figure S3). [d, e] Values of k_{off} were obtained by extrapolation to zero denaturant of the linear dependence (slope m_U) of the logarithm of the rate of dissociation/unfolding on GdmCl concentration (see Figure S6).

ence of k_{on} on ionic strength was predicted for the fastest associating mutant complex, $FimGt^{Q134E\text{-}S138E}/DsF^{T4R\text{-}T6R\text{-}D13N}$. Figure S4 shows that its k_{on} value indeed dropped 10-fold when the ionic strength was increased from 11 mM to 1M, confirming that the enhancement of k_{on} had been achieved through electrostatic attractions between protein and peptide.

The results (Figure 2) showed that Gln134 of FimGt can be regarded a key residue whose substitution by a negatively charged residue was the most efficient, single amino acid replacement in FimGt in accelerating DsF WT binding. To test whether the replacement of additional FimGt residues by acidic residues improved DsF WT binding independently to a similar extent, we produced the double variants $FimGt^{Q134E\text{-}T21E}$, $FimGt^{Q134E\text{-}N22E}$, $FimGt^{Q134E\text{-}Y31E}$, $FimGt^{Q134E\text{-}Q130E}$, and $FimGt^{Q134E\text{-}T132E}$ and recorded the kinetics of DsF WT binding. The k_{on} value remained unchanged for $FimGt^{Q134E\text{-}Q130E}$, slightly decreased for $FimGt^{Q134E\text{-}T21E}$ and $FimGt^{Q134E\text{-}N22E}$, and only increased 1.3-fold compared to $FimGt^{Q134E}$ in the case of $FimGt^{Q134E\text{-}Y31E}$ (Figure S5). $FimGt^{Q134E\text{-}T132E}$ aggregated to higher oligomers during purification and was not investigated further. Thus, there are most likely no additional key positions in FimGt where the introduction of an additional negative charge would lead to an enhancement of the association rate with DsF WT comparable to the Q134E replacement.

We next tested whether the mutations introduced into FimGt and DsF affected the stability of the assembled complexes against spontaneous dissociation/unfolding. As reported for FimGt/DsF WT, none of the mutant complexes spontaneously dissociated under physiological conditions. Their off rates (k_{off}) were therefore determined by extrapolating the dependence of their rates of dissociation/unfolding on denaturant (GdmCl) concentration to zero denaturant (Table 1; Figure S6). As expected from our design approach, the off rates of most mutant complexes stayed within the same range as the k_{off} value of FimGt/DsF WT, and did not increase more than 30-fold for any of the mutant complexes (Table 1). In addition, similar kinetic m_U values (where m_U is given by the slope of the linear dependence of $\ln(k_{off})$ on GdmCl concentration) in the range of 3.8–4.3 M^{-1} were obtained for the mutant complexes, demonstrating that the solvent accessibilities, and hence structures, of the transition states of dissociation/unfolding were similar for all complexes. The fastest associating complex, $FimGt^{Q134E\text{-}S138E}/DsF^{T4R\text{-}T6R\text{-}D13N}$, also proved to be the thermodynamically most stable one: Its kinetic parameters $k_{on} = (2.52\pm0.05)\times10^{4}\,M^{-1}s^{-1}$ and $k_{off} = (2.2\pm0.5)\times10^{-17}\,s^{-1}$ yielded a K_D value of $(8.8\pm2.0)\times10^{-22}$ M. To the best of our knowledge, this is the lowest K_D value ever reported for a noncovalent protein–ligand complex.

The crystal structure of the FimGt/DsF WT complex revealed that Ala1 and residues 13–15 of the DsF peptide are disordered and do not interact with FimGt, while DsF residues 3–12 form ideal β-sheet hydrogen-bonding interactions with the neighboring β-strands of the protein.[6b] This indicated that it should be possible to shorten the DsF peptide at its N- and C-terminus without significant loss of complex stability as long as the backbone–backbone hydrogen-bonding network between the peptide and protein is not affected. To determine the minimum DsF length still sufficient for rapid association and slow dissociation, we systematically shortened $DsF^{T4R\text{-}T6R\text{-}D13N}$ from either terminus and measured

on and off rates with FimGt^{Q134E} (Figures S7, S8, Table S1). We found that removal of the two N- and three C-terminal peptide residues did not impair the k_{off} value by more than two orders of magnitude. Further truncations, which were expected to diminish the hydrogen-bonding network, increased the k_{off} value at least 10-fold for each additionally deleted residue. The most destabilizing effect was observed when C-terminal DsF truncations included Arg12, which increased k_{off} up to 1000-fold (Table S1). The deletion of one N-terminal or the three C-terminal residues had no effect on the k_{on} values. Further deletion of Asp2 increased the k_{on} value 3-fold, whereas deletion of Ser3 and Arg4 did not affect k_{on}. However, deletion of Arg12 decreased k_{on} up to 12-fold. Arg12 is thus a key DsF residue that is essential for both slow dissociation and fast association. Together, the results show that two N- and three C-terminal residues can be removed from DsF$^{T4R\text{-}T6R\text{-}D13N}$ without loss of critical binding characteristics for technical applications, resulting in a 10-residue core peptide with the sequence SRIRIRGYVR (DsF^{SRIRIRGYVR}). To mimic terminal fusions or insertions of DsF^{SRIRIRGYVR} into target proteins in technical applications of the FimGt/DsF system, N-terminally acetylated and/or C-terminally amidated variants of the core peptide were analyzed. Acetylation of the N-terminus led to a 40-fold decrease in k_{off} but was neutral regarding k_{on}, indicating that the positive charge at the free N-terminus in the core peptide does not contribute to electrostatically assisted binding. Amidation of the C-terminal carboxylate however further improved the k_{on} value 3-fold (Table S1).

To complete the kinetic dataset, we measured the on and off rates for the complex between the DsF^{SRIRIRGYVR} core peptide and the FimGt variant FimGt$^{Q134E\text{-}S138E}$ showing fastest binding (Figure S9; see data at the bottom of Table 1). Relative to the binding of full-length DsF$^{T4R\text{-}T6R\text{-}D13N}$ to FimGt$^{Q134E\text{-}S138E}$ and analogous to the results obtained for FimGt^{Q134E}, the k_{on} value increased 3-fold to $(7.8 \pm 0.2) \times 10^4\,\text{M}^{-1}\text{s}^{-1}$. The FimGt$^{Q134E\text{-}S138E}$/DsF^{SRIRIRGYVR} complex thus showed the fastest association rate of all FimGt/DsF variants tested in our study, with a 280-fold higher k_{on} value compared to FimGt/DsF WT. Although its k_{off} was increased 600-fold relative to the most stable complex FimGt$^{Q134E\text{-}S138E}$/DsF$^{T4R\text{-}T6R\text{-}D13N}$, it is still infinitely stable under physiological conditions ($K_D = (1.7 \pm 0.4) \times 10^{-19}$ M). Thus, from a practical point of view, the combination of FimGt$^{Q134E\text{-}S138E}$ with DsF^{SRIRIRGYVR} appears optimal for technical applications of the FimGt/DsF system such as affinity purification.

The observation that the kinetic stabilities of the mutant FimGt/DsF complexes remained extremely high strongly suggested that their three-dimensional structures are similar to that of the WT complex, as expected from our design approach. We solved the crystal structures of the FimGt^{Q134E}/DsF$^{T4R\text{-}T6R\text{-}D13N}$, the FimGt$^{Q134E\text{-}S138E}$/DsF$^{T4R\text{-}T6R\text{-}D13N}$, and the FimGt^{Q134E}/DsF^{SRIRIRGYVR} complex at 1.5, 1.3 and 1.0 Å resolution, respectively (Figure 3; Table S2). A comparison with the structure of the WT complex shows that the folds of all four complexes are highly similar, with root-mean-square deviations (RMSD values) for all Cα atoms of 0.60, 0.54, and 0.50 Å calculated for the pairwise superpositions (Figure 3a). All mutant DsF peptides inserted in the same register and in the antiparallel orientation relative to the C-terminal F strand of FimGt like DsF WT, and adopted highly similar β-strand conformations (Figure S10). Moreover, the shape complementarity of the protein/peptide interface, the interface area, and the intermolecular hydrogen-bonding network were practically unaffected by the amino acid substitutions (Table S3).

We next calculated electrostatic surface potentials for all complexes. In agreement with the nature of the amino acid substitutions and truncations, the introduction of two arginine residues into the peptide sequence generated a basic patch, while removal of Asp2 of the peptide led to the disappearance of an acidic patch. Similarly, but less pronounced, the Q134E and S138E substitutions on the protein side further acidified its surface (Figure 3b). In addition, the newly introduced charges likely led to the formation of additional salt bridges between protein and peptide (Figure S11).

In summary, we achieved an acceleration of the association of the small one-domain protein FimGt and its natural, 15-residue peptide ligand DsF by more than two orders of magnitude using a rational, structure-based engineering approach that generated attractive electrostatic forces between protein and peptide. Only solvent-exposed protein and peptide residues that do not interact in the FimGt/DsF WT complex were selected for amino acid substitutions. As expected, and in agreement with other studies on protein–protein complexes,[5b,c] the dissociation rates of the mutant complexes were not dramatically affected and only increased significantly when the intermolecular hydrogen-bonding network between protein and peptide was diminished by N- or C-terminal truncations in the peptide.

So far, the rational improvement of on rates had only been conducted for complexes between globular proteins.[5] We show herein that this engineering approach works equally well if one of the binding partners is intrinsically disordered. In fact, in agreement with our observations, first examples for natural systems have been described where electrostatics contribute strongly to binding of an intrinsically disordered protein to its globular partner.[9] The accelerated association of FimGt and DsF variants reported here is expected to greatly facilitate practical applications of the system, such as affinity purification of large protein complexes bearing a DsF-tagged subunit, as the incubation times required for quantitative association of DsF-tagged proteins with immobilized FimGt are significantly reduced.

Acknowledgements

This work was supported by the Swiss National Science Foundation (grants 310030B_138657 (to R.G.), 31003A_156304 (to R.G.), and 140879 (to G.C)). We thank Hiang Dreher and the beamline staff of the Swiss Light Source, Villigen, Switzerland for excellent technical assistance. We are also grateful to Spencer Bliven and Kumaran Baskaran for help in the refinement of one of the structures.

Keywords: biophysics · electrostatic interactions · kinetics · protein engineering · protein–protein interactions

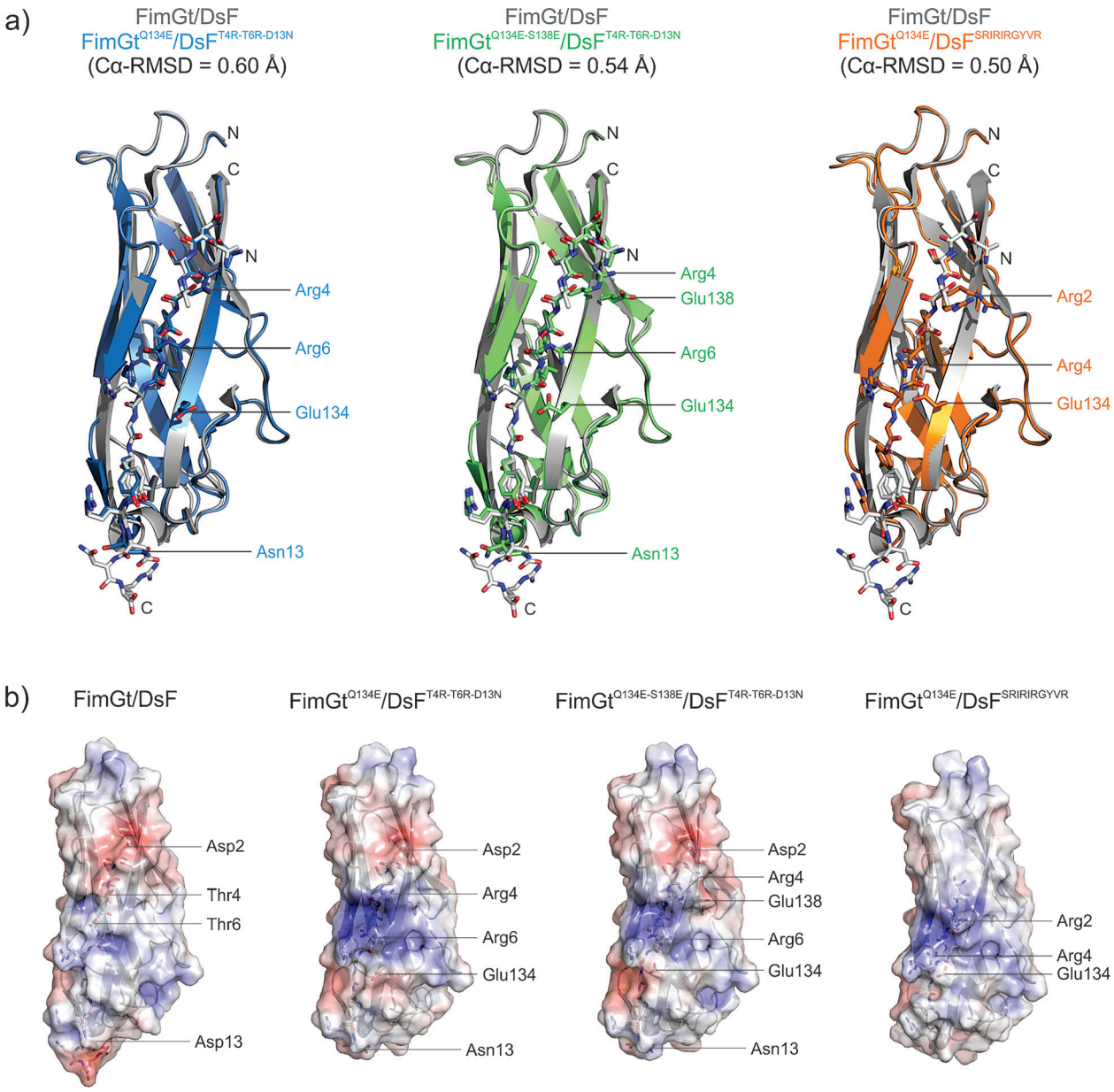

Figure 3. Structural comparison of the FimGt/DsF WT complex and three of the improved complexes. a) Pairwise superpositions of the crystal structure of the FimGt/DsF WT complex (gray, pdb code 3BFQ) with the structure of FimGt^{Q134E}/DsF$^{T4R\text{-}T6R\text{-}D13N}$ (blue, 5IQM, left panel), FimGt$^{Q134E\text{-}S138E}$/DsF$^{T4R\text{-}T6R\text{-}D13N}$ (green, 5IQO, center panel), and FimGt^{Q134E}/DsF^{SRIRIRGYVR} (orange, 5IQN, right panel). DsF peptides are shown as stick models and the corresponding Cα RMSD values are given in brackets. b) Electrostatic surface potentials of the wild type and the three mutant complexes ranging from $+5$ kTe^{-1} (blue) to -5 kTe^{-1} (red). The orientation of the complexes is as in panel (a). The positions of the substituted or truncated residues are indicated.

How to cite: *Angew. Chem. Int. Ed.* **2016**, *55*, 9350–9355
Angew. Chem. **2016**, *128*, 9496–9501

[1] a) J. Dogan, S. Gianni, P. Jemth, *Phys. Chem. Chem. Phys.* **2014**, *16*, 6323–6331; b) S. Qin, X. Pang, H. X. Zhou, *Structure* **2011**, *19*, 1744–1751; c) G. Schreiber, G. Haran, H. X. Zhou, *Chem. Rev.* **2009**, *109*, 839–860; d) Y. Shaul, G. Schreiber, *Proteins* **2005**, *60*, 341–352.

[2] a) O. G. Berg, P. H. von Hippel, *Annu. Rev. Biophys. Biophys. Chem.* **1985**, *14*, 131–160; b) M. v. Smoluchowski, *Z. Phys. Chem.* **1917**, *92*, 129–168.

[3] a) S. H. Northrup, H. P. Erickson, *Proc. Natl. Acad. Sci. USA* **1992**, *89*, 3338–3342; b) M. Schlosshauer, D. Baker, *Protein Sci.* **2004**, *13*, 1660–1669.

[4] a) Z. Radic, P. D. Kirchhoff, D. M. Quinn, J. A. McCammon, P. Taylor, *J. Biol. Chem.* **1997**, *272*, 23265–23277; b) G. Schreiber, A. R. Fersht, *Nat. Struct. Biol.* **1996**, *3*, 427–431; c) S. R. Stone, J. Hofsteenge, *Biochemistry* **1986**, *25*, 4622–4628; d) P. H. von Hippel, O. G. Berg, *J. Biol. Chem.* **1989**, *264*, 675–678; e) D. Walker, G. R. Moore, R. James, C. Kleanthous, *Biochemistry* **2003**, *42*, 4161–4171; f) R. Wallis, G. R. Moore, R. James, C. Kleanthous, *Biochemistry* **1995**, *34*, 13743–13750; g) H. Wendt, L. Leder, H. Harma, I. Jelesarov, A. Baici, H. R. Bosshard, *Biochemistry* **1997**, *36*, 204–213.

[5] a) C. Kiel, T. Selzer, Y. Shaul, G. Schreiber, C. Herrmann, *Proc. Natl. Acad. Sci. USA* **2004**, *101*, 9223 – 9228; b) J. S. Marvin, H. B. Lowman, *Biochemistry* **2003**, *42*, 7077 – 7083; c) T. Selzer, S. Albeck, G. Schreiber, *Nat. Struct. Biol.* **2000**, *7*, 537 – 541.
[6] a) C. Giese, F. Zosel, C. Puorger, R. Glockshuber, *Angew. Chem. Int. Ed.* **2012**, *51*, 4474 – 4478; *Angew. Chem.* **2012**, *124*, 4551 – 4555; b) C. Puorger, O. Eidam, G. Capitani, D. Erilov, M. G. Grutter, R. Glockshuber, *Structure* **2008**, *16*, 631 – 642.
[7] a) D. Choudhury, A. Thompson, V. Stojanoff, S. Langermann, J. Pinkner, S. J. Hultgren, S. D. Knight, *Science* **1999**, *285*, 1061 – 1066; b) M. K. Hospenthal, A. Redzej, K. Dodson, M. Ukleja, B. Frenz, C. Rodrigues, S. J. Hultgren, F. DiMaio, E. H. Egelman, G. Waksman, *Cell* **2016**, *164*, 269 – 278; c) I. Le Trong, P. Aprikian, B. A. Kidd, M. Forero-Shelton, V. Tchesnokova, P. Rajagopal, V. Rodriguez, G. Interlandi, R. Klevit, V. Vogel, R. E. Stenkamp, E. V. Sokurenko, W. E. Thomas, *Cell* **2010**, *141*, 645 – 655; d) F. G. Sauer, K. Futterer, J. S. Pinkner, K. W. Dodson, S. J. Hultgren, G. Waksman, *Science* **1999**, *285*, 1058 – 1061.
[8] M. Nishiyama, T. Ishikawa, H. Rechsteiner, R. Glockshuber, *Science* **2008**, *320*, 376 – 379.
[9] a) D. Ganguly, S. Otieno, B. Waddell, L. Iconaru, R. W. Kriwacki, J. Chen, *J. Mol. Biol.* **2012**, *422*, 674 – 684; b) J. M. Rogers, A. Steward, J. Clarke, *J. Am. Chem. Soc.* **2013**, *135*, 1415 – 1422.

Received: April 14, 2016
Published online: June 28, 2016

